

Analysis of bonded tubular single lap joints subjected to varying pressure at constant torsion

The effect of internal pressure coupled with torsion on the bonded socket joints with laminated FRP composite pipes as adherents has been studied in the present research. Influence of internal pressure conditions which are most commonly experienced during flow of various fluids, has been taken into account under constant torsion. Finite element method (FEM) based modelling and simulation technique, capable of detailing the three-dimensional stresses along with fracture analysis of the bonded joint has been used. The effect of pressure on the adherend-adhesive interfaces, which are vulnerable to adhesion failure has been analyzed through the modelling technique.

Keywords: Adhesion failure, FEM, FRP composite, torsion.

I. Introduction

Composite piping systems involving use of fiber-reinforced polymer (FRP) composites are becoming increasingly popular in the engineering applications as alternative to conventional engineering materials.

The unique characteristics of FRP, such as their light weight, their resistance to corrosion, high energy absorption, and the lower cost of transportation, erection and maintenance are the promising key factors in various engineering fields.

Mining industry has been successfully replacing steel pipes with composite pipes thereby paving way for environmental friendly fluid transportation systems.

Increased study into joining techniques is crucial to effectively manage component repairs as well as carrying out upgrades and expansions of composite piping systems, thereby elevating the reliability of operation and repair of these systems to a level commiserate with industrial requirements.

With the advancement of adhesive materials and

techniques in adhesive bonding in the past decades, a number of adhesively bonded joint systems have been increasingly applied in engineering structures, such as the single-lap joint, single-strap joint, double lap joint and pipe joint in aeronautics, automotive, civil engineering structures etc.

There is a need to investigate the effect of internal pressure combined with torsion on the performance of pipe joint, adhesive layers as well as adherend-adhesive interfaces. Special attention has been devoted to study the effect of pressure increase at constant torsion on the failure prone regions.

II. Specimen geometry and boundary conditions

Fig.1 shows geometry, configuration, loading and boundary conditions of the bonded TSLJ specimen analyzed in the present study. Two Gr/E [0]4 laminated FRP composite tubes which are similar with respect to length, thickness, and properties have been used as adherents. Here zero degree fibre orientation indicates circumferentially wound fibres. The two tubes have been joined through a thin layer of adhesive (epoxy) as shown in the Fig.1.

The bonded TSLJ have been subjected to an internal pressure of 10 MPa at the inner adherent as well as torsion loading of 100 N-m (direction of the applied torque is CCW as we see from the free end of the bonded TSLJ) at the free end of the bonded TSLJ structure.

Internal pressure loading has been varied as 1MPa, 10MPa, 13 MPa, and 16 MPa for a constant torsional loading of 100 N-m in order to study the effect of circumferential pressure variation on joint strength.

The material properties along with strength values for adhesive and adherents have been given in Table 1. The material properties have been considered from then work of Das and Pradhan [2].

Three different bondline interfaces have been identified to be the critical regions prone to stress concentration effects in the present analysis: (i) inner adherend-adhesive interface, (ii) adhesive mid-layer, and (iii) outer adherend-adhesive interface (Fig.1). Two-dimensional stress distribution comparison in different cases has been over viewed.

Messrs. R. R. Das, Deptt. of Mining Machinery Engineering, Indian School of Mines, Dhanbad, Jharkhand. E-mail: ramakanta.pratima@gmail.com and N. Baishya and V. Ranjan, School of Mechanical Engineering, Kalinga Institute of Technology, Bhubaneswar, Odisha, India. E-mail: nayanjyoti.baishya@gmail.com

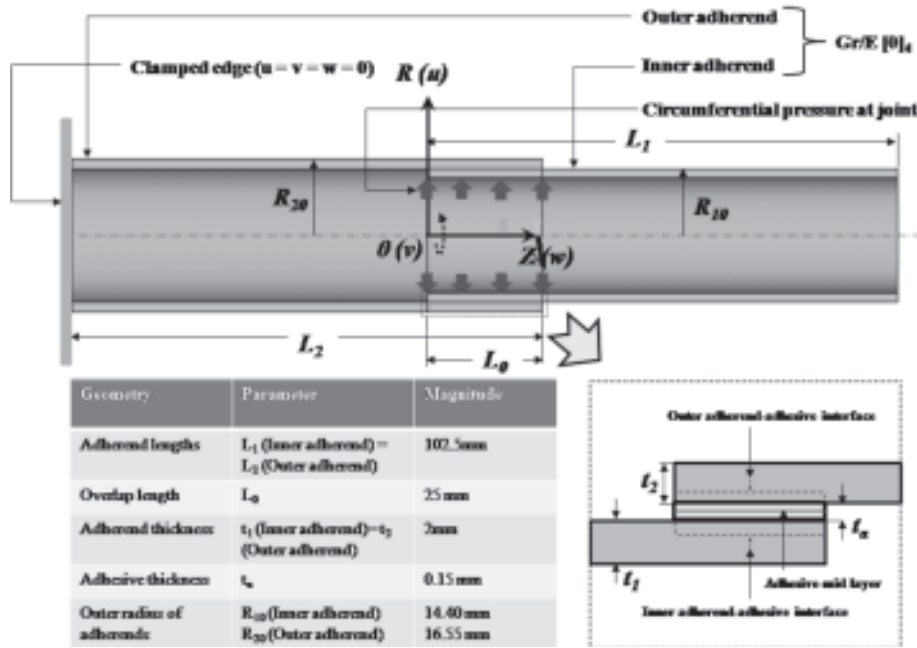


Fig.1 Specimen geometry and boundary conditions of the bonded socket joint along with different interfaces at the joint region

As per the conclusions made by Das and Pradhan [2] a zero gap has been considered in the present analysis. Overlap length/socket length (L_0) and adhesive thickness (t_a) have been considered as the joint parameters which need to be optimized for improved performance of the bonded TSLJ under influence of axial and circumferential pressure loading.

In search for the optimized joint parameters, the overlap length/socket length (L_0) has been varied from 20 mm to 45 mm. Similarly the adhesive thickness (t_a) has been varied from 0.1 to 1 mm thickness in the present investigation. However, during the starting of the analysis an overlap/socket length of 20 mm and an adhesive thickness of 0.1 mm has been considered.

III. Finite element modelling

The bonded TSLJ has been modelled using the FE codes of ANSYS 14.0. The FE mesh of the bonded TSLJ specimen has been shown in Fig.2. Solid brick 8-node 185 elements of ANSYS FE package have been used for modelling both the FRP composite adherends and the epoxy adhesive layer.

TABLE I: GRAPHITE/EPOXY FRP COMPOSITE LAMINA AND EPOXY ADHESIVE MATERIAL PROPERTIES

	Material constants	Strengths
T300/934 graphite/epoxy FRP composite adherend:	$E_z = 127.5$ GPa, $E_0 = 9$ GPa	$Z_T = 1586$ MPa
	$E_r = 4.8$ GPa	$Z_C = 1517$ MPa
	$\nu_{r0} = \nu_{rz} = 0.28$ $\nu_{0z} = 0.41$	$\theta_T = \theta_C = 80$ MPa
	$G_{r0} = G_{rz} = 4.8$ GPa	$R_T = R_C = 49$ MPa
	$G_{0z} = 2.55$ GPa	$S_{0r} = S_{zr} = 2.55$ MPa
		$Y_T = 65$ MPa $Y_C = 884.5$ MPa
Epoxy adhesive:	$E = 2.8$ GPa, $\nu = 0.4$	

These elements provide the advantage of simulating both structural and layered elements.

A very fine mesh has been adopted to take care of high stress gradients at the free edges of the joint. The element size in the overlap region has been considered to be 1 parts \times 120 parts \times 125 parts for both the adherend and adhesive layer. However for the portion of the tubular adherends laying outside the overlap region a comparatively coarse mesh has been adopted. For better results the meshing pattern has been made comparatively finer towards the joint and course towards the free and fixed edges (Fig.2)

IV. Results and discussion

Three dimensional stress distributions within the joint region of the bonded TSLJ have been studied in details for pure internal pressure loading and pure torsional loadings. In the present chapter effect of internal pressure loading on the stress distributions

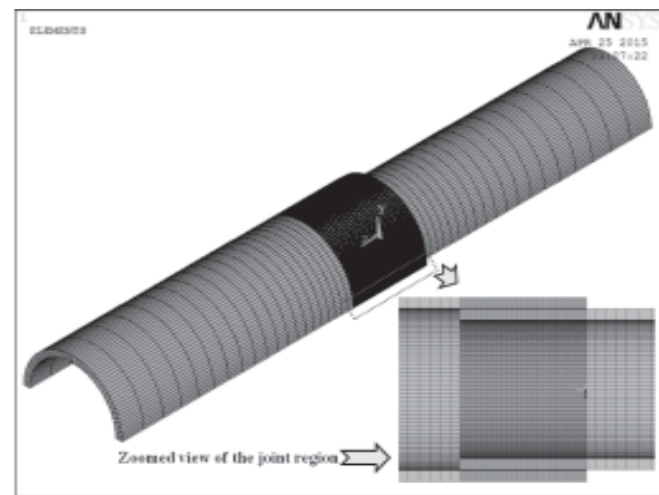


Fig.2 Finite element mesh of the bonded tubular single lap joint along with zoomed view of the meshing pattern around the joint region

within the joint region is intended to be studied when the bonded TSLJ is already under the application of a torsional loading at the free end. Effect of internal pressure (10 MPa) on stress distributions and failure indices at different bondline interfaces of the bonded TSLJ subjected to a torsional loading of 100 N-m has been studied in the first phase of the analysis.

Thereafter, the pressure has been increased as: 1MPa, 10MPa, 13 MPa, and 16 MPa for a constant torsional loading of 100 N-m and effects have been studied corresponding to the critical bondline interface.

A. EFFECT OF INTERNAL PRESSURE IN PRESENCE OF TORSION ON STRESSES IN JOINT

1. Inner adherend-adhesive interface

It has already been observed in Fig.3 that under influence of internal pressure the normal stresses (σ_r , σ_θ , and σ_z) at the inner adherend-adhesive interface are of considerable magnitude. Whereas, the shear stresses ($\tau_{r\theta}$, $\tau_{\theta z}$) are of comparatively negligible magnitude, except the axial-radial shear stress (τ_{rz}). Similarly, under pure torsional loading, all the shear stresses ($\tau_{r\theta}$, $\tau_{\theta z}$) are of considerable magnitudes except the radial axial shear stress (τ_{rz}). The present case is just a superposition of these two cases. The stress distributions also seem to be following a superposition trend as seen from Fig.3.

Introduction of internal pressure loading in the joint region enhances the magnitude of normal stresses (σ_r , σ_θ , and σ_z) and the axial-radial shear stress (τ_{rz}) within the inner adherend-adhesive interface of the bonded TSLJ (Fig. 3 (a), (b), and (c)). It could be clearly observed that the profile of these stresses (σ_r , σ_θ , σ_z , and τ_{rz}) matches exactly with the corresponding stress profiles for pure pressure loading case (Fig. 3 (a), (b), (c), and (f)). This confirms that the stress distributions follow the superposition principle. Similarly the shear stress profiles ($\tau_{r\theta}$, $\tau_{\theta z}$) have been observed to be

unaffected due to introduction of internal pressure loading in presence of the torsional loading. The stress profiles again match exactly with the profiles corresponding to pure torsional loading case (Fig.3 (d), (e)) confirming the superposition principle again.

2. Adhesive mid-layer

Introduction of internal pressure loading of 10 MPa in the joint region enhances the magnitude of normal stresses (σ_r , σ_θ , and σ_z) and the axial-radial shear stress (τ_{rz}) within the adhesive mid-layer of the bonded TSLJ (Fig. 4 (a), (b), and (c)).

It could be clearly observed that the profile of these stresses (σ_r , σ_θ , σ_z , and τ_{rz}) matches exactly with the corresponding stress profiles for pure pressure loading case (Fig. 4 (a), (b), (c), and (f)).

This confirms that the stress distributions follow the superposition principle.

Similarly the shear stress profiles ($\tau_{r\theta}$, $\tau_{\theta z}$) have been observed to be unaffected due to introduction of internal pressure loading in presence of the torsional loading. The stress profiles again match exactly with the profiles corresponding to pure torsional loading case (Fig.4 (d), (e)) confirming the superposition principle again.

3. Outer adherend-adhesive interface

When an internal pressure loading of 10 MPa has been introduced in the joint region in presence of torsional loading acting at the free end of the bonded TSLJ, it enhances the magnitude of normal stresses (σ_r , σ_θ , and σ_z) and the radial-

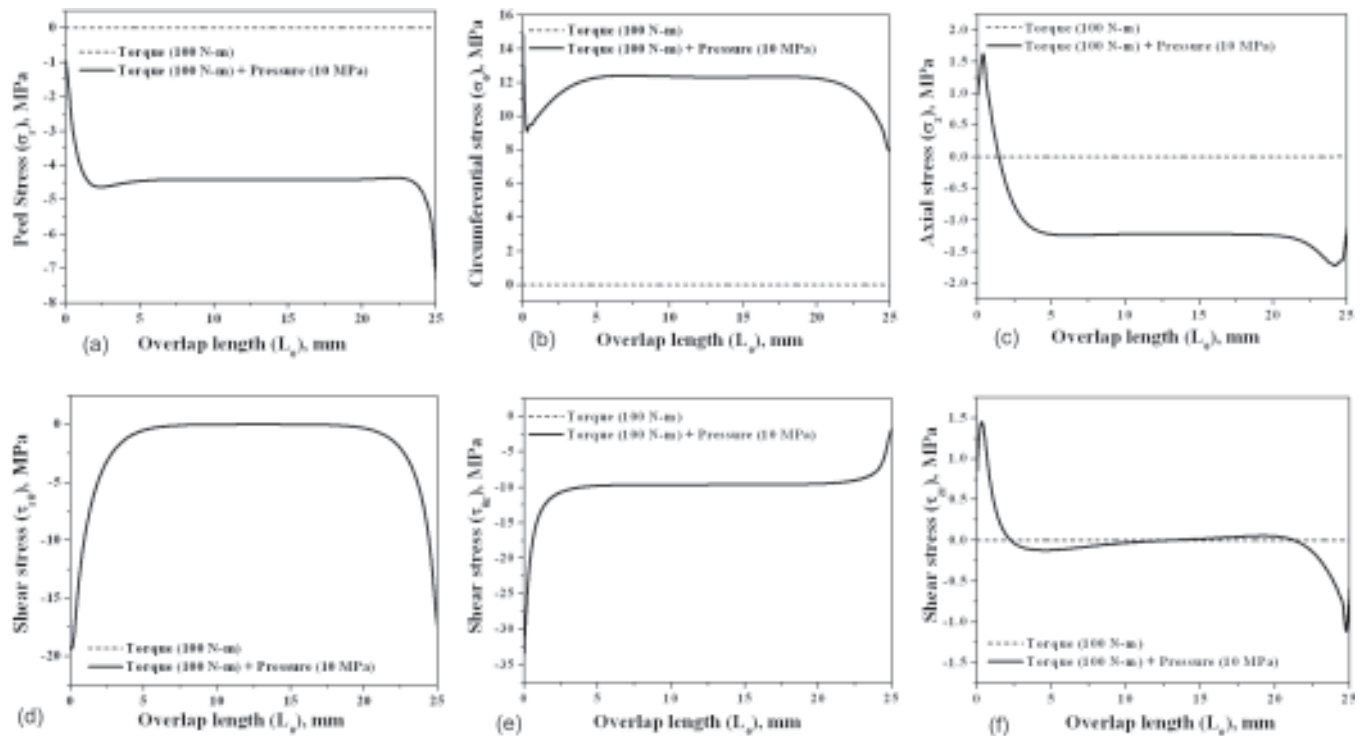


Fig.3 Effect of introduction of circumferential pressure in presence of torque on stress distributions at the inner adherend-adhesive interface

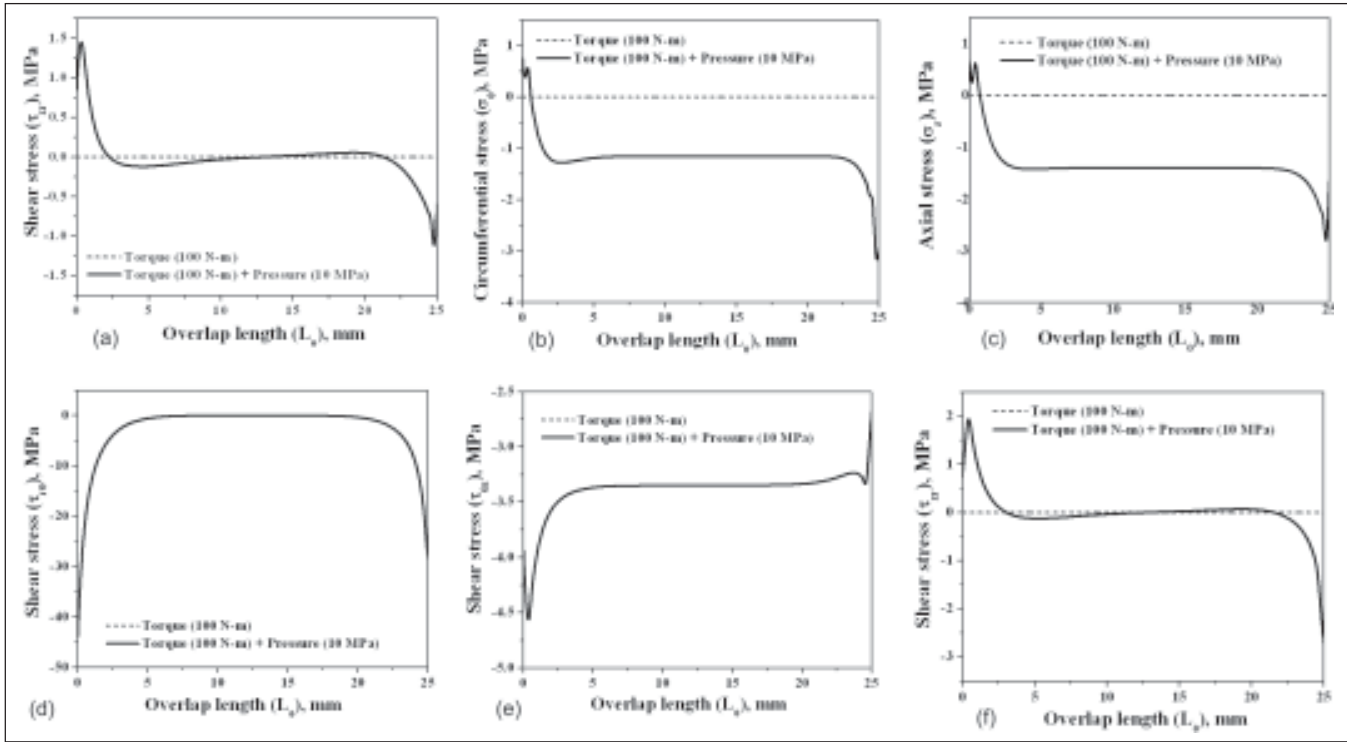


Fig.4 Effect of introduction of circumferential pressure in presence of torque on stress distributions at the adhesive mid-layer

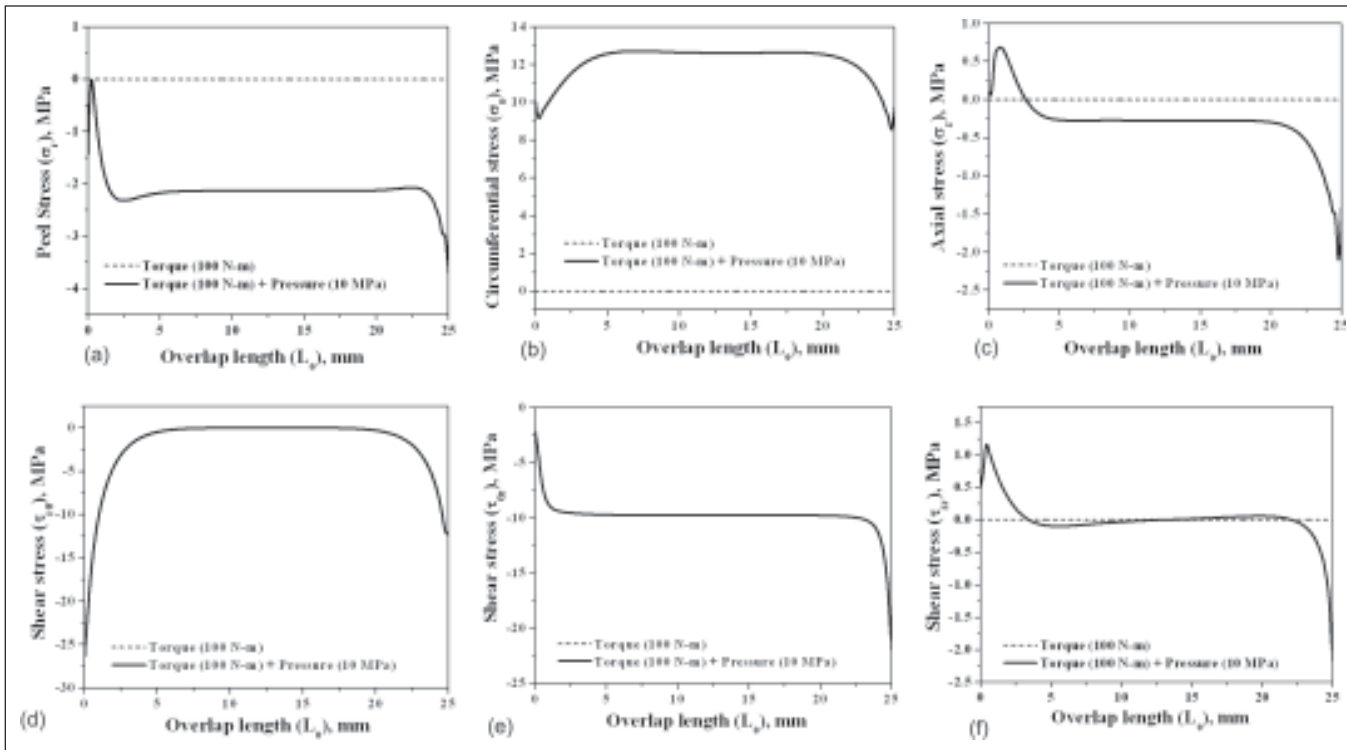


Fig.5 Effect of introduction of circumferential pressure in presence of torque on stress distributions at the outer adherend-adhesive interface

axial shear stress (τ_{rz}) within the outer adherend-adhesive interface (Fig.5 (a), (b), and (c)).

It could be clearly observed that the profile of these stresses (σ_r , σ_θ , σ_z , and τ_{rz}) matches exactly with the

corresponding stress profiles for pure pressure loading case (Fig. 5 (a), (b), (c), and (f)).

This confirms that the stress distributions follow the superposition principle. Similarly the shear stress profiles ($\tau_{r\theta}$,

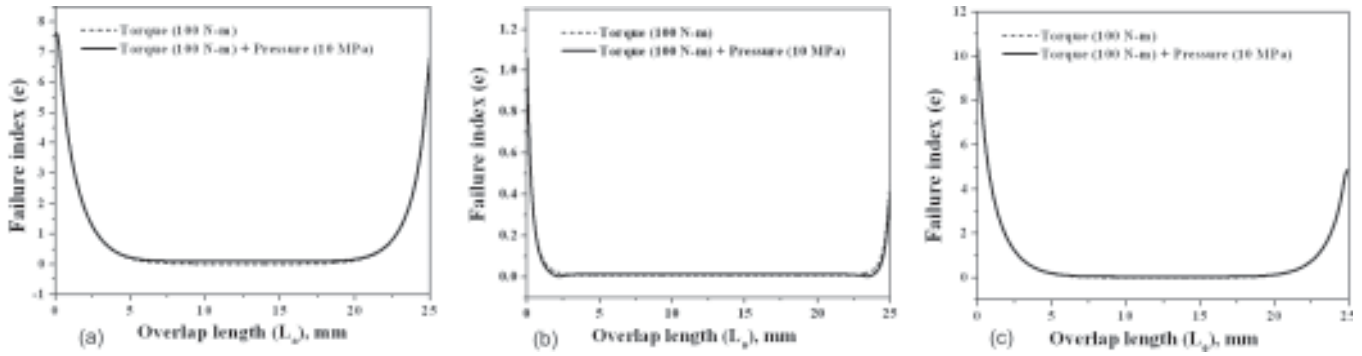


Fig.6 Effect of introduction of circumferential pressure in presence of torque on failure indices at different bondline interfaces: (a) inner adherend-adhesive interface, (b) adhesive mid-layer, and (c) outer adherend-adhesive interface

$\tau_{\theta z}$) have been observed to be unaffected due to introduction of internal pressure loading in presence of the torsional loading. The stress profiles again match exactly with the profiles corresponding to pure torsional loading case (Fig.5 (d), (e)) confirming the superposition principle.

B. EFFECT OF INTERNAL PRESSURE IN PRESENCE OF TORSION ON FAILURE WITHIN JOINT

It can be marked that failure index profiles for pure pressure and pressure and torque combined are almost coinciding with each other (Fig.6).

The failure index trends for all the bondline interfaces are matching exactly with the failure index trends corresponding to pure torsional loading as shown in Fig. 6. This indicates that introduction of internal pressure along with the pure

torsional loading is not affecting the failure index profiles for the different bondline interfaces. Hence the outer adherend-adhesive interface remains the critical bondline interface under this combined loading which is prone to fail through adhesion failure towards the clamped edge (as in the case of pure torsional loading).

C. EFFECT OF PRESSURE VARIATION IN PRESENCE OF TORSION ON STRESSES IN THE CRITICAL BONDLINE INTERFACE

As the pressure has been varied from 1MPa to 16 MPa in presence of a constant torque of 100 N-m, it can be observed that only the normal stress components (σ_r , σ_θ , and σ_z) and the radial-axial shear stress (τ_{rz}) component have been increasing. However, the remaining shear stress components ($\tau_{r\theta}$, $\tau_{\theta z}$) have remained unchanged due to the pressure variation (Fig.7).

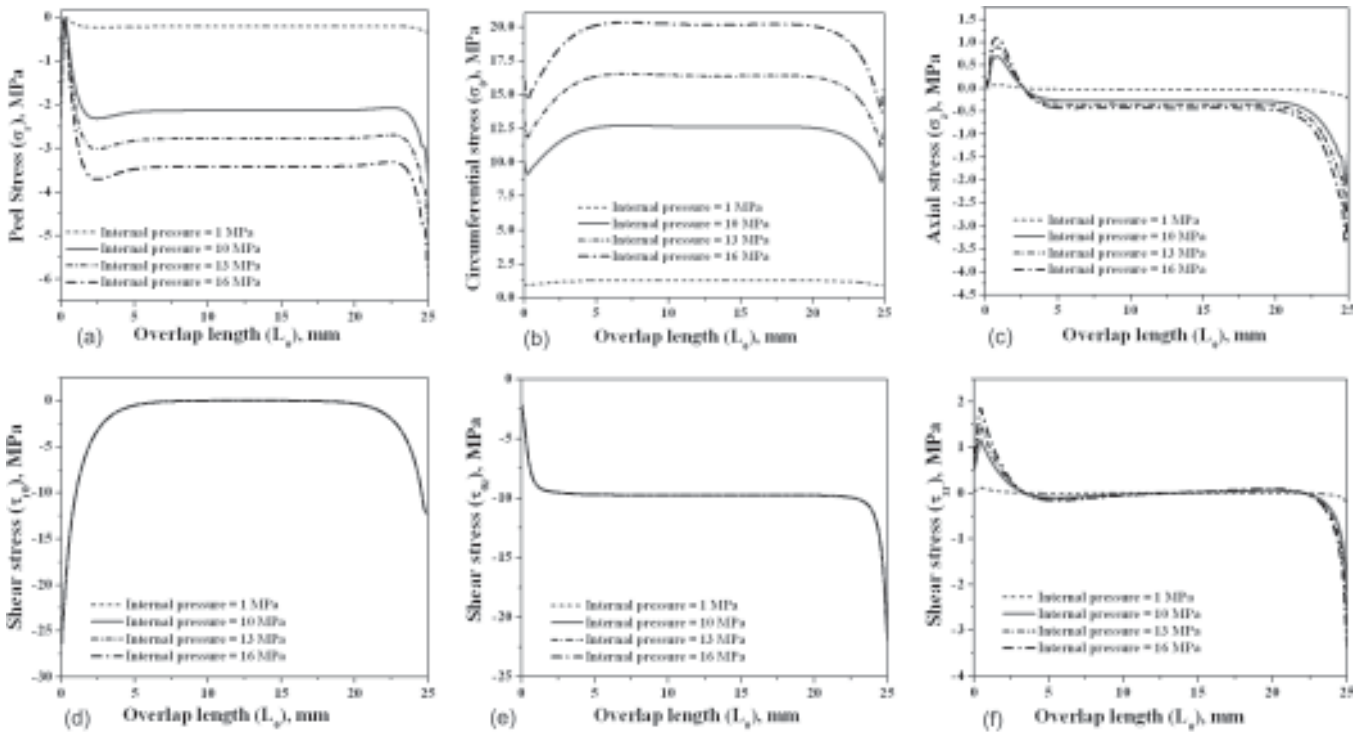


Fig.7 Effect of increase in circumferential pressure in presence of torque on stress distribution within the outer adherend-adhesive interface

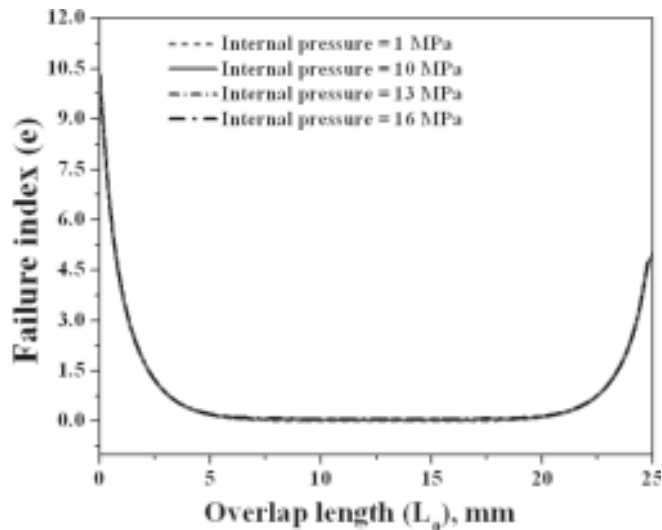


Fig.8 Effect of increase in circumferential pressure in presence of torque on failure within the outer adherend-adhesive interface

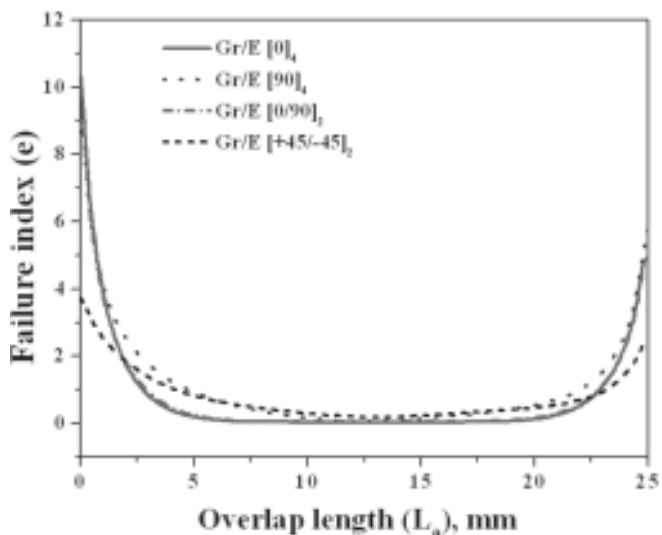


Fig.9 Effect of stacking sequences on Tsai-wu coupled stress criteria based failure indices at critical bondline interface under combined pressure and torsional loading

D. EFFECT OF PRESSURE VARIATION IN PRESENCE OF TORSION ON FAILURE AT THE CRITICAL BONDLINE INTERFACE

Although variation of internal pressure at constant torsion has got impact on the stress distribution at the outer adherend-adhesive interface (Fig.7), but it has got negligible effect on the failure index values as shown in Fig. 8. So increase in internal pressure has got negligible effect on the failure at the critical bondline interface. It has been observe from the given plot that variation in magnitude of internal pressure not showing a desirable effect on the failure. It can be clearly seen from failure index plot that on a small increment in pressure value, the failure indices are almost coinciding with other and also the pressure with lower magnitude found to be safe towards failure indices.

E. EFFECT OF DIFFERENT PLY-ORIENTATIONS ON FAILURE AT THE CRITICAL BONDLINE INTERFACE DUE TO VARIATION OF PRESSURE AT CONSTANT TORSION

It is interesting to note that, as internal pressure is introduced in presence of torsional loading Gr/E [+45/-45]₂ ply-orientations seem to be better as it reduced the magnitude of failure indices corresponding to the critical bondline interface (Fig.9). The circumferentially wound fiber orientation (Gr/E [0]₄) and axially cross-ply orientation (Gr/E [0/90]₂) which have been found to be better corresponding to pure pressure and pure torsional loading have been observed to be giving comparatively greater failure index values. Hence for a combined torsional and pressure loading the angle ply-orientation (Gr/E [+45/-45]₂) is most preferable.

V. Summary and conclusions

Laminated FRP composite made bonded TSLJ subjected to a constant torsion (100 N-m) and varying internal pressure loading (1 MPa to 16 MPa) has been analyzed through finite element method. The FE codes have been developed through ANSYS APDL in a high speed IBM platform. Stress and failure effects within the joint region have been studied carefully in presence and absence of internal pressure (along with torsional loading). Finally effect of different ply orientations on the failure indices corresponding to the critical bondline interface has been studied and a suitable stacking sequence has been suggested for an improved performance of the joint. The salient conclusions have been enlisted below.

- Four stress (σ_r , σ_θ , σ_z , and τ_{rz}) components within all the bondline interfaces have been enhanced considerably (maintain the same magnitude as in the case of pure pressure loading) due to introduction of internal pressure loading along with a constant torsional loading.
- However, the remaining stress components ($\tau_{r\theta}$, $\tau_{\theta z}$) remain unaltered (maintain the same magnitude as in the case of pure torsional loading) due to introduction internal pressure loading along with a constant torsional loading.
- Introduction of internal pressure along with the pure torsional loading is marginally affecting the failure index profiles for the different bondline interfaces.
- Outer adherend-adhesive interface is the critical bondline interface which is prone to fail through adhesion failure towards the clamped edge under combined pressure and torsional loading (as in the case of pure torsional loading).
- As the pressure has been varied, four stress components (σ_r , σ_θ , σ_z , and τ_{rz}) within the joint have been increasing. However, the remaining shear stress components ($\tau_{r\theta}$, $\tau_{\theta z}$) have remained unchanged.
- Increase in internal pressure has got negligible effect on the failure at the critical bondline interface (outer adherend-adhesive interface).

(Continued on page 217)

8. Chaboche, J. L. and Lesne, P. M. (1988): "A non-linear continuous fatigue damage model," *Fatigue and Fracture of Engineering Materials and Structures*, vol.11(1), pp.1-7, 1988.
9. Lemaitre, J. and Plumtree, A. (1979): "Application of damage concepts to predict creep-fatigue failures," *ASME Journal of Engineering, Materials and Technology*, vol.101, pp.284-292, 1979.
10. Socie, D. F., Fash, J. W. and Leckie, F. A. (1983): "A continuum damage model for fatigue analysis of cast iron," In *Advances in Life Prediction Methods*, ed, D. A. Woodford and J. R. Whitehead. The American Society of Mechanical Engineers, New York, pp. 59-64, 1983.
11. Hua, C. T. and Socie, D. F. (1984): "Fatigue damage in 1045 steel under constant amplitude biaxial loading," *Fatigue of Engineering Materials and Structures*, vol. 7(3), pp.165-179, 1984.
12. Lemaitre, J. and Chaboche, J. L. (1978): "Aspect phenomenologique de la rupture par endommagement," *Journal Mecanique Appliquee*, vol. 2(3), pp.317-365, 1978.
13. Wang, J. (1992): "A continuum damage mechanics model for low-cycle fatigue failure of metals," *Engineering Fracture Mechanics*, vol. 41(3), pp.437-441, 1992.
14. Wang, T. and Lou, Z. (1990): "A continuum damage model for weld heat affected zone under low cycle fatigue loading," *Engineering Fracture Mechanics*, vol.37 (4), pp.825-829, 1990.
15. Chow, C. L. and Wei, Y. (1991): "A model of continuum damage mechanics for fatigue failure," *International Journal of Fracture*, vol.50, pp.301-316, 1991.
16. Wang, June (1992): "A Continuum Damage Mechanics Model For Low-Cycle Fatigue Failure Of Metals," *Engineers Fracture Mechanics*, vol. 41(3), pp. 437-441, 1992.
17. Yang, Xiaohua, Li, Nian, Jin, Zhihao and Wang, Tiejun (1997): "A continuous low cycle fatigue damage model and its application in engineering materials," *Int. J. Fatigue*, Vol. 19(3) pp. 687-692, 1997.
18. Xiao, Y.-C., Li, S. and Gao, Z. (1998): "A continuum damage mechanics model for high cycle fatigue," *Int. J. Fatigue*, vol. 20(7), pp. 503-508, 1998.
19. Bhattacharya, Baidurya and Ellingwood, Bruce (1998): "Continuum damage mechanics analysis of fatigue crack initiation," *Int. J. Fatigue*, vol. 20(9), pp. 631-639, 1998.
20. Upadhyaya, Y. S. and Sridhara, B. K. (2012): "Fatigue life prediction: A continuum damage mechanics and fracture mechanics approach," *Materials and Design*, vol.35, pp.220-224, 2012.
21. Bonora, N. and Newaz, G. M. (1998): "Low cycle fatigue life estimation for ductile metals using a nonlinear continuum damage mechanics model," *Int. J. Solids Structures*, Vol. 35(16), pp. 1881-1894, 1998.
22. Shang, De-Guang and Yao, Wei-Xing (1999): "A nonlinear damage cumulative model for uniaxial fatigue," *International Journal of Fatigue*, vol. 21, pp.187-194, 1999.
23. Jesus, Abilio M. P. De, Riberio, Alfredo S. and Fernandes, Antonio A. (2005): "Finite element modeling of fatigue damage using continuum damage mechanics," *Journal of Pressure Vessel Technology*, vol.127, pp.157-164, 2005.
24. Dattoma, V., Giancane, S., Nobile, R. and Panella, F. W. (2006): "Fatigue life prediction under variable loading based on new non-linear continuum damage mechanics model," *International Journal of Fatigue*, vol. 28, pp.89-95, 2006.

FATIGUE DAMAGE ESTIMATION THROUGH CONTINUUM DAMAGE MECHANICS

(Continued from page 213)

- ◆ For a combined torsional and pressure loading the angle ply-orientation (Gr/E [+45/-45]2) is most preferable.

References

1. Zou, G. P. and Taheri, F. (2006): "Stress analysis of adhesively bonded sandwich pipe joints subjected to torsional loading" *Int. J. Solids Struct.* 43, 5953-5968 (2006).
2. Das, R. R. and Pradhan, B. (2011): "Finite Element Based Design and Adhesion Failure Analysis of Bonded Tubular Socket Joints Made with Laminated FRP Composites," *J. Adhes. Sci. Technol.* 25, 41-67 (2011).
3. Lees, J. M. (2004): Combined pressure/tension behaviour of adhesive-bonded GFRP pipe joints. In: Hollaway LC, Chryssanthopoulos MK, Moy SSJ, editors. *Advanced polymer composites for structural applications in construction*, ACIC. Woodhead Publishing Ltd; p. 377-383, (2004).
4. Panigrahi, S. K. and Pradhan, B. (2007): "Delamination damage analyses of adhesively bonded lap shear joints in laminated FRP composites," *International Journal of Fracture*, 148, pp. 373-385 (2007).
5. Esmael, R. A. and Taheri, F. (2009): "Influence of adherend's delamination on the response of single lap and socket tubular adhesively bonded joints subjected to torsion" *J Adhes Sci Technol*, 23 p. 1827-1844 (2009).